LUNAR GRAVITY FIELD DETERMINATION

W. Flury

European Space Operations Centre (ESOC)
Darmstadt
Federal Republic of Germany

ABSTRACT

The current status of the lunar gravity field determination is reviewed and then followed by a discussion of the POLO (= Polar Orbiting Lunar Observatory) gravity experiment. The mission baseline comprises two spacecraft: the Orbiter in a low-altitude, near-circular polar orbit and the Relay in a high-altitude trajectory. The two-spacecraft concept allows Doppler tracking on the lunar farside (via Relay) and improves the coverage in the polar regions. Covariance analysis shows that processing of Relay Doppler data permits an order-of-magnitude improvement of the precision of the polar moment of inertia parameter. To this end, daily tracking sessions of two hours over 27 days are required. Doppler data accurate to 1-2 mm/s is essential.

Keywords: Lunar Gravity Field, Moment of Inertia, Doppler Tracking, Covariance Analysis.

1. INTRODUCTION

A new era in the exploration of our closest neighbour in space, the moon, began with the launch of Luna 1 on January 2, 1959. To date 46 probes have been launched, the most recent being Luna 24 (launched 9 August 1976). An unprecedented amount of information was gathered from the flybys, orbiters and landers.

One of the physical aspects of the moon is the gravity field. Besides the importance of gravity on the dynamics, the external gravity field, together with topographic, librational and seismic data, sets boundary constraints on models of the lunar interior. Gravity and topographic models of equivalent resolution allow the calculation of Bouguer gravity anomalies, a necessary prerequisite for the study of isostatic compensation in crust and upper mantle. The possible existence of a lunar core can be inferred from precise gravity data, although current evidence is inconclusive.

1.1 Methods for lunar gravity field determination

The foremost data source pertaining to the lunar gravity field are the lunar orbiters. Gravity field anomalies cause variations of the spacecraft velocity, which can be observed by the Doppler frequency shift of a radio signal transponded or emitted from the spacecraft. The Doppler signal is proportional to the relative velocity in the direction between spacecraft and ground-station.

Three methods of processing Doppler data for gravity field determination are (1) direct dynamic modeling, (2) long-term orbit evolution, and (3) line-of-sight accelerations.

In the classical approach (method 1), spacecraft epoch state and gravity coefficients are simultaneously estimated adopting a weighted least-squares scheme. An initial estimate of epoch state, gravity coefficients and possibly some other parameters (solar radiation pressure) is differentially corrected until the sum of the weighted least squares of the Doppler residuals becomes stationary. With this approach, which involves numerical integration of the spacecraft equations of motion and the associated variational equations, spherical harmonic coefficients through thirteenth degree and order were determined (Ref. 1).

Method 2 is a two-step approach. Method 1 is first applied to short data arcs to derive a set of mean elements. In a second step the gravity parameters are obtained from the long-period and secular variations of the mean elements, which is a linear estimation problem. The advantage of method 2 is the computational ease to handle data arcs of long duration (several months). Examples of this method are Refs. 2 (complete to degree and order sixteen) and 3 (complete to degree and order seven, zonals to degree twelve).

Method 3 is a two-step procedure to determine local gravity features. Method 1 is first applied to short data arcs adopting a low degree and order gravity model. The resulting Doppler residuals contain the high-frequency gravity field information.

Proc. Int. Symp. Spacecraft Flight Dynamics, Darmstadt, FRG, 18-22 May 1981 (ESA SP-160, Aug. 1981)

Spline fitting and differentiation of the residuals leads to line-of-sight (LOS) accelerations. Contours of LOS accelerations on lunar topographic charts allow the identification of local gravity features, such as mascons (Ref.4) or craters. A subsequent step is to fit LOS accelerations to local mass distributions using a least-squares scheme (Ref. 5). Application of method 3 for quantitative geophysical modeling is cumbersome, since LOS accelerations are biased because of the least square procedure of orbit determination. Ref. 6 reports 25-30% amplitude compression and peak anomaly shift.

LOS acceleration is most valuable when the line-of-sight coincides with the local vertical.

1.2 The current knowledge of the lunar gravity field

Characteristic for the lunar gravity field are the relatively mild broad-scale variations and the distinct local gravity features such as mascons and craters. This particular structure requires a large number of terms in the spherical harmonic expansion of the gravity potential.

A fundamental deficiency of all lunar gravity models is related to the lack of data on the lunar farside and the inhomogeneous data distribution on the front side. Attempts to reduce the deleterious effect of sparse or lacking data with a priori covariances are problematical since the solution is preconditioned on constructed data.

Recent gravity models were derived from data of the Apollo missions 8, 12, 15 and 16; the Apollo subsatellites 15 and 16; the Lunar Orbiters 1, 2, 3, 4 and 5; and Explorer 35 (AIMP-E) and 49 (RAE-B). The Lunar Orbiters were either in low inclination ($<30^{\circ}$) or nearly polar orbits. Explorer 35 was placed in an eccentric, retrograde orbit (a=5980 km, e=0.576, $i=170^{\circ}$). The Explorer 49 orbit was: a=2803 km, e=0.002 and $i=62^{\circ}$.

Evidence of the unsatisfactory knowledge of the lunar gravity field is the radial acceleration error at 100 km altitude. Ref. 2 quotes formal acceleration errors between 30 and 65 milligals (1 milligal = 10^{-3} cm s^{-2}). As expected, the error is maximum on the lunar farside and in the polar regions.

A term-by-term comparison of two solutions, Ref. 2 and 7, both complete to sixteenth degree and order, illustrates the difficulties involved in determining the lunar gravity field from existing data. Second- and third-degree coefficients are reliably determined while already the estimates for J_5 have a different sign. The formal uncertainty exceeds the estimate already for some fifth-degree coefficients.

A carefully designed mission, such as POLO, could remove many uncertainties and misconceptions and advance significantly our knowledge of the lunar gravity field. The next section describes the objectives of the POLO gravity experiment, followed by results of a covariance analysis, which dealt with the Relay gravity analysis.

2. THE POLO GRAVITY EXPERIMENT

The mission baseline comprises two spacecraft: the Orbiter in a low-altitude (100 km), near-circular polar orbit and the Relay in a high-altitude trajectory (Fig. 1). Doppler links ground-station to Orbiter and Relay, and Relay to Orbiter are assumed to exist.

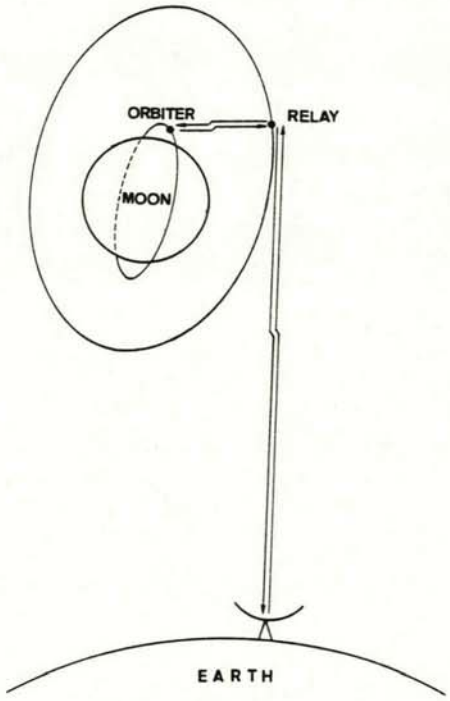

Fig. 1 POLO Mission Geometry

The scientific objectives of POLO are described in Ref. 8. The primary goals of the gravity experiment are:

(1) identification of local gravity models

(2) global high-resolution gravity survey

(3) improved determination of low degree and order harmonics

(4) improved determination of C/MR^2.

2.1 Identification of local gravity models

The objective is to determine gravity models of local features (up to 250 km extension) to an accuracy of 5 milligals.

The first step is to compute LOS accelerations from the raw Doppler data. Contour lines of LOS accelerations on lunar topographic maps allow the detection of gravity anomalies. Bouguer gravity anomalies will be determined from free-air-gravity anomalies by treating topography above the selenoid as equivalent gravity.

In the past this technique was restricted to the lunar frontside excluding polar regions. The link Orbiter to Relay will permit a global application.

2.2 Global high-resolution gravity survey

The objective is to obtain a global high-resolution map (200 km resolution, 5-10 milligal accuracy) of the lunar gravity field using the Doppler link earth to Orbiter and the bent-pipe link via Relay.

The anomalous gravity potential may be represented as

$$\Delta U = \frac{\mu}{r} \sum_{n=1}^{\infty} \sum_{m=o}^{n} \left(\frac{R}{r}\right)^n P_n^m \quad (\sin\beta)$$

$$\{C_{nm} \cos m\lambda + S_{nm} \sin m\lambda\}$$

where μ denotes the lunar gravitational constant, r the selenocentric radius, β the selenographic longitude, λ the selenographic longitude, R the mean lunar radius, and P_n^m the associated Legendre functions. By convention the zonal coefficients are $J_n = -C_{n,o}$ and $S_{n,o} = 0$.
The task is to estimate the C_{nm} and S_{nm}.

2.3 Improved determination of low degree and order harmonics

The objective is to improve the estimates of the low degree and order harmonics from the Doppler link earth to Relay. The Relay orbit, if properly chosen, will only be sensitive to the long wavelength components of the gravity field, and consequently, the gravity solution will not be aliased by higher order terms.

2.4 Improved determination of C/MR^2

Let A, B and C denote the principal moments of inertia. The principal axes of minimum moment A and maximum moment C have mean directions which deviate slightly from the mean earth and mean rotation direction.

The polar moment of inertia parameter is linked to C_{20} or C_{22} by

$$\frac{C}{MR^2} = \frac{2C_{20}\ (1+\beta)}{\gamma-2\beta-\beta\gamma} = \frac{4C_{22}}{\gamma},$$

where M = lunar mass, $\beta = \frac{C-A}{B}$ and $\gamma = \frac{B-A}{C}$.
The fractional differences in the moments β and γ play a role in the lunar physical librations. They are rather accurately determined from lunar laser ranging.

C/MR^2 is related to the internal structure of the moon. The moment of inertia parameter of a solid homogeneous sphere is 0.4. Lower values indicate a density increase towards the center. Thus precise estimates of C/MR^2 allow boundary conditions for a possible core (density and dimension) to be established.

A recent estimate (Ref. 9) is 0.391 ± 0.002 based on $\sigma_\beta = 0.03 \times 10^{-6}$, $\sigma_\gamma = 0.7 \times 10^{-6}$ and $\sigma_{C_{20}} = 0.9^{\beta} \times 10^{-6}$.
Assuming a core radius of 300 km, this uncertainty of C/MR^2 corresponds to a core density variation of about 4 g/cm^3, which is too large to be geophysically significant.

The limiting factor for a precise determination of C/MR^2 is the uncertainty of the gravity coefficients. The error of C/MR^2 is plotted in Figs 2 and 3 as a function of the errors of C_{20}, C_{22} and γ. In Fig. 2 $\sigma_\beta = \sigma_\gamma$ was assumed.

$$\frac{C}{MR^2} = \frac{2C_{20}(1+\beta)}{\gamma - 2\beta - \beta\gamma}$$

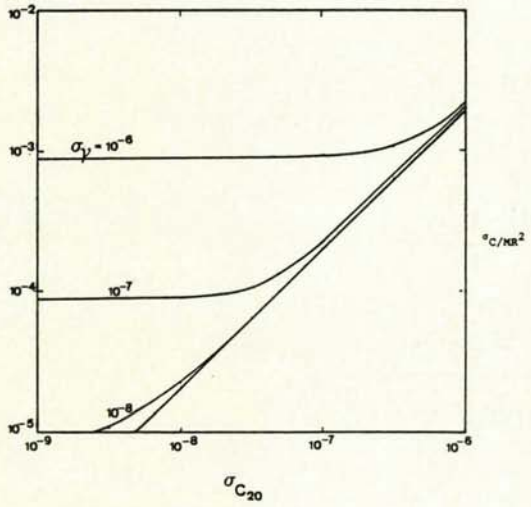

Fig. 2 UNCERTAINTY IN C/MR^2

$$\frac{C}{MR^2} = \frac{4C_{22}}{\gamma}$$

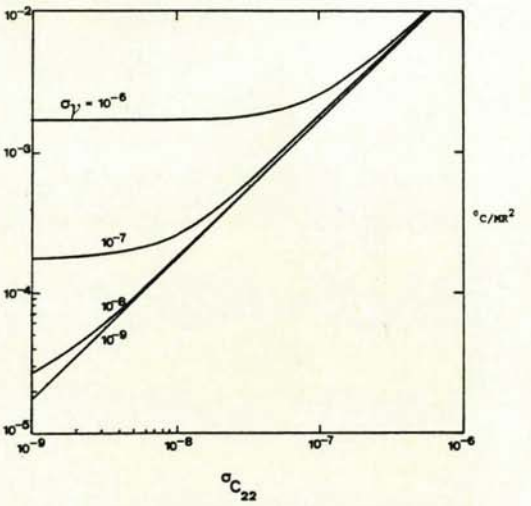

Fig. 3 UNCERTAINTY IN C/MR^2

The goal of POLO is an order-of-magnitude improvement of the precision of C/MR^2. This can be achieved by either improving the estimate of C_{20} or C_{22}, but then γ has to be known with an accuracy of about 10^{-7} which can be expected from lunar laser ranging. Ref. 10 quotes errors on β and γ derived from libration models of 1.32×10^{-7} and 1.00×10^{-7}, respectively.

The remainder of this paper is concerned with the improved determination of C/MR^2 and low degree and order harmonics. Covariance analyses are performed assuming Doppler tracking of the Relay from two ground-stations.

3. THE RELAY ORBIT

The Relay spacecraft has to fulfill two main functions:

(1) serve as relay station for the bent-pipe Doppler link

(2) provide suitable Doppler data for the determination of the long-wavelength gravity variations.

Eccentric orbits are ruled out for the following reason: they are sensitive to a large number of gravity harmonics around the periapsis, yet the information content of Doppler data is insufficient for their determination. The optimum choice is a near-circular orbit with main perturbations arising from the low degree and order harmonics and strongly attenuated effects of high-frequency terms. Studies carried out at JPL and ESOC (Ref. 11, 12) concluded 5000 km to be the appropriate altitude.

G. Janin (Ref. 13) discovered a most interesting strategy to attain such an orbit. Both spacecraft, Orbiter and Relay, are inserted into lunar transfer orbit in a mated configuration. Separation occurs after injection into a selenocentric polar orbit with perilune and apolune altitudes of 100 km and 10000 km, respectively. The Orbiter reaches its circular orbit with a further impulse at periselenium. The perturbation of the earth decreases the eccentricity of the Relay orbit for suitable initial values of the argument of periselenium. This strategy does not demand a separate propulsion capability for the Relay and may be an optimum solution from the point of view of system complexity. The disadvantage is a delay of at least 150 days until the eccentricity is reduced to appropriate values. A typical time history of the eccentricity is displayed in Fig. 4a. From $e_o = 0.73$ the eccentricity reaches the minimum of 0.07 after 320 days. Subsequently, the eccentricity increases until the orbit decays after about 1000 days. Fig. 4b illustrates the sensitivity of the eccentricity decrease with respect to the initial value of the argument of periselenium. The ordinate is the eccentricity after 235 days and the abscissa the deviation of ω from the optimum value. The long-term variation of the semi-major axis is negligible.

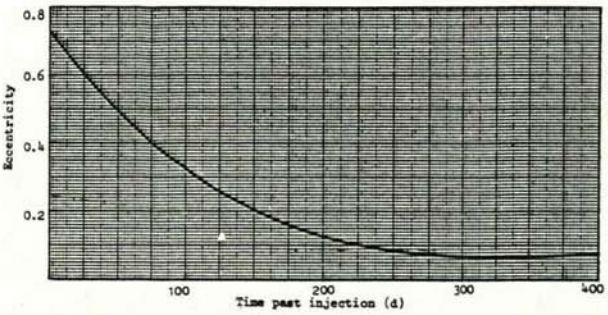

Fig. 4a Eccentricity vs time

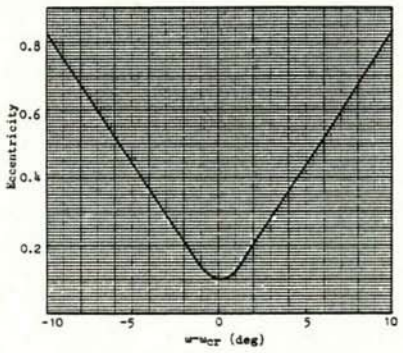

Fig. 4b Eccentricity 235 d past injection vs $\omega - \omega_{cr}$

This concept of the "natural circularization" of the Relay orbit is feasible. The coverage of the lunar farside is not impeded by an eccentric Relay orbit (Ref. 14). The only negative aspect, as compared to an immediate circularization, is the five months waiting period, after which a reliable determination of low degree and order spherical harmonics becomes possible.

4. COVARIANCE ANALYSIS

4.1 Assumptions

4.1.1. Ground-stations. Two ground-stations are considered, Weilheim and Carnarvon. Their coordinates are given in Table 1.

	E Longitude (deg.)	Latitude (deg.)
Carnarvon	113.72	-24.90
Weilheim	11.08	47.88

Table 1 Ground-station Coordinates

Station coordinates within a global reference frame can be determined with 1-2 m accuracy (i.e. a Doppler campaign of the Transit system). According to Ref. 11 station location errors of 10 m do not affect the precision of the estimate. Therefore, errors of this type were ignored.

4.1.2 The Dopler observable. The Doppler observable provides the velocity of the spacecraft relative to the ground-station. The basic measurements are range differences over Doppler count times. Differentiation yields averaged values of the relative velocity. Since the variance of the measurement noise is inverse proportional to the count time, a trade-off between measurement accuracy and resolution can be made.

Irrespective of one-way or two-way Doppler, a random error of the range-rate measurements of 0.3-10 mm/s (1σ) is assumed.

4.1.3 Relay orbit. A "naturally circularized" Relay orbit is assumed. Table 2 gives the orbit parameters at insertion and at the times when the eccentricity has decreased to 0.2 and 0.1, respectively.

epoch	1.1.1987	14.6.1987	1.9.1987
time since injection (d)	0	165	244
semi-major axis (km)	6788.09	6788.09	6788.09
periapsis altitude (km)	100	3691.2	4371.4
apoapsis altitude (km)	10000	6408.8	5728.6
eccentricity	0.7292	0.2	0.1
inclination (deg)	90	88.68	89.09
longitude of ascending node (deg)	184.95	188.88	190.22
argument of periapsis (deg)	141.0	138.18	135.02

Table 2 Relay Orbit Parameters

The lunar equator defines the fundamental plane. The longitude of the ascending node is measured from the ascending node of the lunar orbit on the lunar equator (Cassini point).

4.1.4 Gravity error model. We take as a priori statistics of the estimated gravity coefficients Kaula's rule of thumb. It finds for the terrestrial gravity field the standard deviation for the normalized coefficients of degree n to be $\sigma_n = 10^{-5}/n^2$. The extrapolation to other planets is effected by assuming that the strength of supporting material is similar to that of the earth and that equal stresses are supported. The condition of equal stresses implies a scaling factor

$$f = \left(\frac{M_p}{M_E}\right)^2 \left(\frac{R_E}{R_p}\right)^4 ,$$

where M_E and M_p are the masses, and R_E and R_P the radii of earth and planet, respectively. Kaula's rule gives for the expected absolute values of the unnormalized harmonic coefficients (δ_{om} is the Kronecker symbol)

$$|C_{nm}, S_{nm}| = \frac{1}{f} \sqrt{\frac{(n-m)!\ (2n+1)(2-\delta_{om})}{(n+m)!}}\ \frac{10^{-5}}{n^2}$$

The lunar value of f is 0.027. Kaula's rule provides a pessimistic estimate for the a priori errors of the gravity coefficients.

For unadjusted gravity coefficients the more realistic error statistics from Ref. 2 are adopted. Both a priori statistics are listed in Table 3.

n	m	Kaula's rule of thumb $\sigma_{C_{nm}}$, $\sigma_{S_{nm}}$	Ferrari (1977) $\sigma_{C_{nm}}$	Ferrari (1977) $\sigma_{S_{nm}}$
2	0	210	3.8	-
2	2	60	1.2	1.4
3	0	110	12	-
3	1	44	1.6	1.8
3	2	14	1.3	1.6
3	3	5.7	.99	.95
4	0	69	.39	-
4	1	22	1.7	1.7
4	2	5.2	.98	.69
4	3	1.4	.31	.31
4	4	.49	.10	.099
5	0	49	7.4	-
5	1	13	.68	.96
5	2	2.4	.45	.39
5	3	.49	.21	.20
5	4	.12	.047	.038
5	5	0.36	.0015	.022
6	0	37	7.0	-
6	1	8.1	3.3	.28
6	2	1.3	.61	.67
6	3	.21	.079	.076
6	4	.039	.025	.027
6	5	.0083	.0051	.0053
6	6	.0024	.0013	.0014
7	0	29	18	-
7	1	5.5	2.2	2.2
7	2	.75	.43	.48
7	3	.11	.081	.078
7	4	.016	.0081	.0080
7	5	.0027	.0020	.0022
7	6	.00052	.00044	.00044
7	7	.00014	.00012	.00012

Table 3 A Priori Errors of Unnormalized Harmonic Coefficients ($\times 10^6$)

4.2 Covariance algorithm

This study utilizes a linear error analysis program which simulates weighted least squares processing of Doppler data in batch mode.

Let z denote the vector of data residuals (observed-computed). We assume z to be linearly related to the solve-for parameters x and the consider variables y by

$$z = Ax + By + \eta$$

where $A = \frac{\partial z}{\partial x}$, $B = \frac{\partial z}{\partial y}$ and η is the data noise vector. x represents corrections to the estimated parameters. The y variables remain unadjusted, only their uncertainty is "considered". The dimensions are z = (m x 1), A = (m x n), B = (m x p), y = (p x 1) and η = (m x 1).

The computed covariance of the estimate $\hat{x}$ of x is

$$C = E\left[(\hat{x} - x)\ (\hat{x} - x)^T\right] = (A^T W A + C_o^{-1})^{-1}$$

where W is the data weight matrix and C_o the a priori covariance.

In the case of a minimum variance estimate W is the inverse noise covariance matrix:

$$W^{-1} = E(\eta\eta^T).$$

For uncorrelated noise with standard deviation σ_n the weight matrix may be expressed as

$$W = \frac{1}{\sigma_n^2} I,$$

I = unit matrix.

The computed covariance takes only the effect of data noise into account and ignores any systematic error due to the consider variables y. A more realistic measure of the estimation error is the consider covariance which includes the uncertainty of the y parameters. Assuming that the errors in the y parameters are uncorrelated with the data noise, the consider covariance is

$$C_c = C + SC_y S^T$$

where C_y = covariance matrix of y

$S = -CA^T WB$ = sensitivity matrix of the error in the estimate of x to the y parameters.

The consider covariance comprises a noise contribution and an unadjusted parameter contribution. In most practical situations the consider variables are the dominating factor.

4.3 Results

The solve-for variables were selected as

- position and velocity of the Relay at epoch;
- gravity harmonic coefficients of degree 2, 3 and 4 (without C_{21} and S_{21}).

The consider variables are

- gravity harmonic coefficients of degree 5 and 6.

The basic data collection period of 27 days was split into three sub-arcs of 9 days duration. After each sub-arc the statistics of the epoch state and the harmonic coefficients are computed.

Unless otherwise stated the a priori Relay state error is

50 km along each coordinate axis
10 m/s along each coordinate axis

for each sub-arc.

Both ground-stations measure the relative velocity to the Relay at the specified sampling rate whenever the spacecraft is visible.

4.3.1 Near-polar orbit, eccentricity ≤ 0.1. The low-eccentric orbit from Table 2 is investigated first ($e \leq 0.1$). The different cases of the covariance analysis are summarized in Table 4. Intermediate results for C_{20} and C_{22} (after each sub-arc) are not shown, only the final ones. Data collection over 27 days turned out to be essential.

Study Case	Data Noise (mm/s)	Sampling Period (minutes)	$\sigma_{C_{20}}$		$\sigma_{C_{22}}$	
			Computed	Consider	Computed	Consider
1	1	1	7.2×10^{-8}	5.6×10^{-7}	6.8×10^{-9}	2.9×10^{-8}
1a	1	1	7.2×10^{-8}	2.9×10^{-7}	6.8×10^{-9}	1.5×10^{-8}
1b	1	1	7.2×10^{-8}	1.1×10^{-6}	6.8×10^{-9}	5.6×10^{-8}
1c	1	1	7.2×10^{-8}	5.6×10^{-7}	6.8×10^{-9}	2.9×10^{-8}
2	1	1	1.1×10^{-7}	5.6×10^{-7}	9.3×10^{-9}	3.0×10^{-8}
3	1	1	9.5×10^{-8}	5.7×10^{-7}	1.0×10^{-8}	3.1×10^{-8}
4a	10	1	7.2×10^{-7}	9.1×10^{-7}	6.8×10^{-8}	7.3×10^{-8}
4b	0.3	1	2.2×10^{-8}	5.6×10^{-7}	2.0×10^{-9}	2.8×10^{-8}
5	1	2	7.2×10^{-8}	5.6×10^{-7}	6.8×10^{-9}	2.9×10^{-8}
6a	1	1	2.1×10^{-7}	5.7×10^{-7}	1.8×10^{-8}	3.7×10^{-8}
6b	1	2	2.9×10^{-7}	6.0×10^{-7}	2.5×10^{-8}	4.1×10^{-8}
7	1	1	3.4×10^{-7}	7.9×10^{-7}	2.7×10^{-8}	4.1×10^{-8}
8a	1	2	2.9×10^{-7}	3.4×10^{-7}	1.5×10^{-8}	2.2×10^{-8}
8b	1	2	2.9×10^{-7}	9.1×10^{-6}	1.5×10^{-8}	6.4×10^{-8}

Table 4 Study Cases

Explanation and comments:

Case 1. All measurements are taken whenever the Relay is visible. Sampling rate is 1 measurement per station every minute.

Case 1a. Only 50% of the a priori statistics of the consider-variables is taken. A linear response of the a posteriori statistics (consider) is observed. The formal statistics remain unaffected.

Case 1b. The a priori statistics of the consider-variables are multiplied by 2. Again the response is linear.

Case 1c. The epoch state a priori was reduced to 5 km in position and 1 m/s in velocity. No effect on the final result.

Case 2. Only Weilheim data is processed.

Case 3. Only Carnarvon data is processed. Both cases, #2 and #3, show similar results as the 2-station solution #1.

Case 4a. Data noise is increased to 10 mm/s. Obviously, the formal statistics are linear to data noise (long data-arc). The consider statistics are degraded by a factor 2-3.

Case 4b. Data noise is reduced to 0.3 mm/s. The consider statistics remain almost unaffected.

Case 5. Reduced sampling rate (1 meas. every 2 minutes). Same accuracy as with 1 meas. every minute.

Case 6a. Each station collects data only for two hours per day. The estimation error of C_{22} increases by about 30%, while C_{20} remains unchanged.

Case 6b. Same as 6a but the sampling rate is reduced to one measurement every 2 minutes. The consider-statistics of C_{20} and C_{22} increase.

Case 7. Each station collects data only for one hour per day. The consider-statistics increase by about 40% compared with case # 1 or # 5 .

Case 8a. The solve-for variables are Relay state and harmonic coefficients from degree 2 to 5. Consider variables are degree 6 and 7 coefficients. Data is collected over 27 days whenever the Doppler link is established. Compared with the previous cases smaller differences between formal and consider statistics are found. But also the "consider" errors themselves are decreased, which shows that the selected Relay Doppler data still contain some information on the fifth-degree harmonics. The optimum splitting between solve-for and consider variables may further reduce the estimation errors.

Case 8b. Same as 8a but the lunar gravitational constant was added to the consider variables. The uncertainty of μ was assumed as 0.005 km^3/s^2. The C_{20} estimation error increases by a factor 20-30 compared to # 8a. C_{22} is less affected, the uncertainty is larger by a factor 3. The deleterious effect of $\delta\mu$ on the C_{20} estimation error has a straightforward explanation. C_{20} causes a secular perturbation of the mean motion. Thus $\delta\mu$ and C_{20} affect the spacecraft position along its orbit qualitatively in the same way and discrimination between the two causes becomes extremely difficult. If the uncertainty of μ cannot be further reduced then the use of C_{20} to calculate moment of inertia parameters becomes questionable. The adopted value for $\delta\mu$ may be too large. Ref. 10, which combined Doppler-data from Lunar Orbiter 4 and lunar laser ranging data, claims a precision of 0.0029 km^3/s^2.

All effort should be made to improve the estimate of μ. One possibility is to process Doppler data from the earth-moon transfer phase. A precise estimate depends however strongly on uninterrupted data arcs (no thruster activation).

The uncertainty of C/MR^2 using C_{22} is 0.4×10^{-3} (# 8a) and 1.2×10^{-3} (# 8b).

As an example of the achievable accuracy with which the low degree gravity coefficients can be determined, the results of study case # 8a (Table 4) are displayed in Table 5. We recall that in # 8a gravity coefficients from degree 2 to 5 are estimated.

n	m	$\sigma_{C_{nm}}$		$\sigma_{S_{nm}}$	
		computed	consider	computed	consider
2	0	.29	.34	-	-
2	2	.15	.022	.037	.061
3	0	1.6	2.1	-	-
3	1	.33	.43	.35	.43
3	2	.18	.19	.16	.19
3	3	.038	.048	.031	.038
4	0	4.2	6.1	-	-
4	1	.20	.41	.26	.30
4	2	.094	.17	.21	.36
4	3	.017	.032	.017	.030
4	4	.0016	.0084	.0016	.0090
5	0	20	26	-	-
5	1	3.6	4.7	4.2	5.3
5	2	.76	.81	.70	.78
5	3	.14	.21	.12	.16
5	4	.0080	.0099	.0081	.010
5	5	.0018	.0024	.0017	.0024

Table 5 A Posteriori Errors of Unnormalized Harmonic Coefficients (x 10^6)

An immediate conclusion from Table 5 is that the Relay orbit is well suited for the determination of the second, third and fourth degree harmonics. The improvement of the fifth degree coefficients is less pronounced.

One should however bear in mind that these results were obtained by processing data over 27 days. A better recovery of the potential coefficients may be achieved with the analysis of the long-term orbit evolution (several months).

4.3.2 Near-polar orbit, eccentricity $\leq$ 0.2. The orbit analyzed in the previous section was obtained 244 days after epoch.

165 days after epoch the eccentricity reaches 0.2. Collecting Doppler data already from day # 166 onwards yields the following results (Weilheim and Carnarvon, sampling period 2 minutes, tracking period 27 days):

	$\sigma_{C_{20}}$	$\sigma_{C_{22}}$
Computed	1.0×10^{-7}	2.7×10^{-8}
Consider	4.9×10^{-7}	9.0×10^{-8}

Thus the estimation error (consider) of C_{20} is smaller, that of C_{22} significantly larger compared with case # 5 of Table 4.

4.3.3 80^0 Inclination, eccentricity $\leq$ 0.1. For a polar orbit the regression of the node due to oblateness vanishes. Only the secular perturbations of the argument of perigee and of the mean longitude are exploited to determine C_{20}.

An obvious question is whether a non-polar orbit would lead to a better determination of C_{20}.

The following orbit is therefore considered:

epoch	1.1.1987	8.9.1987, 23 h
time since injection (d)	0	251
semi-major axis (km)	6788.09	6788.09
periapsis altitude (km)	100	4371.3
apoapsis altitude (km)	10000	5728.9
eccentricity	0.7292	0.1
inclination (deg)	80	82.68
longitude of ascending node (deg)	184.95	180.9
argument of periapsis (deg)	141.0	150.0

Table 6 Relay Orbit Parameters ($I \sim 80^0$)

Processing Doppler data from Weilheim and Carnarvon during 27 days (sampling period = 2 minutes) leads to the following estimation errors:

	$\sigma_{C_{20}}$	$\sigma_{C_{22}}$
Computed	2.7×10^{-7}	7.3×10^{-9}
Consider	1.2×10^{-6}	2.8×10^{-8}

Thus C_{20} is less accurately determined (compared to $I \sim 90^0$) while C_{22} is slightly better estimated.

In this case Doppler data were only collected after the eccentricity had dropped below 0.1.

5. CONCLUSION

1. Doppler tracking of the Relay from two well-separated stations (in longitude) over 27 days leads to an improved determination of the long wavelength variations of the lunar gravity field and of the moment of inertia parameter. A precision of at least 4×10^{-4} in C/MR^2 should be possible. Critical orbit parameters are the semi-major axis ($\sim$7000 km) and the eccentricity (<0.1).

2. The measurement noise was assumed as 1 mm/s. Slightly higher values might also be acceptable. Station location errors were ignored.

3. The accuracy of the estimated gravity coefficients depends critically on the statistics of the consider variables, i.e. the higher degree harmonic coefficients and the lunar gravitational constant.

   After collection of sufficient tracking data (10-20 days) the estimation error is almost proportional to the statistics of the consider-variables and slightly sensitive to higher data rates.

4. Of extreme importance, however, is the total time span during which tracking occurs. Daily tracking periods of 2 hours for each station over 27 days are sufficient for an improved gravity determination.

5. Perturbations of the Relay orbit by thruster operations should be avoided. Manoeuvre-free periods of about 9 days are acceptable.

6. In most of the study cases the gravity coefficients of degree 2-4 were estimated, while degree 5 and 6 coefficients were considered.

   By estimating also fifth degree coefficients, the estimation errors of C_{20} and C_{22} were significantly reduced, which indicates that the selected orbit is still sensitive to higher degree harmonics.

   The selection of the optimum set of solve-for variables is a task still to be carried out.

7. The results cited above were obtained with a near-polar and near-circular orbit ($e_o \sim 0.1$). Data collection began 244 days after insertion into the lunar capture orbit. Processing data from day # 165 onwards ($e_o \sim 0.2$) leads to a significantly larger estimation error of C_{22}.

8. The inclination of the Relay orbit is not a critical parameter. Inclinations of 80^0 and 90^0 lead to similar results.

9. Critical is the lunar gravitational parameter. If the uncertainty of 0.005 km^3/s^2 cannot be further reduced then estimates of C_{20} will be strongly corrupted. The estimate of C_{22} is less affected and can still be used for the determination of the moment of inertia parameter.

   An improved estimate of μ may be obtained from the analysis of Doppler data from the earth-moon transfer phase.

6. REFERENCES

1. Michael H M 1972, Recent results on the mass, gravitational field and moments of inertia of the Moon, *The Moon* 3, 388-402.

2. Ferrari A J 1977, Lunar Gravity: a harmonic analysis, *J Geophys. Res.* 82, 3065-3084.

3. NAS 5-22849 1978, *Lunar gravity analysis from long period orbit evolution*, by Williamson R G.

4. Muller P M & Sjogren W L 1968, Mascons: lunar mass concentrations, *Science*, 161, 680-684.

5. Phillips R J et al 1978, Simulation gravity modeling to spacecraft-tracking data: analysis and application, *J Geophys. Res.* 83, 5455-5464.

6. Gottlieb P 1970, Estimation of local lunar gravity features, *Radio Sci.* 5, 301-312.

7. Bills B G & Ferrari A J 1980, A harmonic analysis of lunar gravity, *J Geophys. Res.* 85, 1013-1025.

8. SCI(79)7, 1979, *Polar Orbiting Lunar Observatory (POLO)*, ESA.

9. Blackshear W T & Gapcynsky J P 1977, An improved value of the lunar moment of inertia, *J Geophys. Res.* 82, 1699-1701.

10. Ferrari A J et al 1980, Geophysical parameters of the earth-moon system, *J Geophys. Res.* 85, 3939-3951.

11. Ananda M P et al 1977, An improved lunar moment of inertia determination: a proposed strategy, *The Moon* 17, 101-120.

12. Flury W 1979, Determination of the lunar moments of inertia, MAD W.P. no. 89, ESOC.

13. Janin G, The stability of eccentric polar orbits around the moon, to be presented at the XXXIInd IAF Congress, Rome, 6-22 Sept. 1981.

14. Janin G et al 1980, POLO Orbiter coverage, MAO W.P. no. 133, ESOC.